REVIEWED

# Characterization and Calibration of a Power Regenerative Hydrostatic Wind Turbine Test Bed using an Advanced Control Valve

Biswaranjan Mohanty and Kim A. Stelson

University of Minnesota
Department of Mechanical Engineering, 111 Church Street SE, Minneapolis, MN, USA
E-Mail: mohan035@umn.edu, kstelson@umn.edu

A hydrostatic transmission is commonly used in off road construction equipment for its high power density. It can also be used in wind turbines for more reliable and cost effective transmission than a conventional gearbox. A power regenerative test platform has been built at the University of Minnesota to understand the performance of a hydrostatic transmission in a wind turbine. In this paper the use of an advanced control valve to characterize the components of the test bed has been demonstrated. The electrohydraulic valve has precise control on pressure and flow and gives more flexibility to the testbed.

**Keywords:** hydrostatic transmission, wind turbine, efficiency, calibration
**Target audience:** Mobile Hydraulics, Mining Industry, Renewable Energy

## 1 Introduction

The global demand for wind energy is increasing rapidly. The worldwide wind capacity has reached 456 MW at the end of June 2016, which is 4.7% of the world's electricity [1]. The US Department of Energy (DOE) has a target of generating 20% of the nation's electricity by 2030 [2]. Most large wind turbine farms are far away from the point of use, increasing transmission cost. In contrast, distributed wind relies on small and mid-size turbines installed at or near the point of use. This reduces the transmission loss and makes the distributed grid more reliable and stable.

A multi stage fixed ratio gearbox is used in a conventional turbine to transmit power from the low speed rotor to the high speed generator. Studies conducted by the National Renewable Energy Laboratory show that electrical systems fail frequently but with shorter downtimes, but gearboxes and generators fail less frequently but with longer downtimes [3][4]. The failure of gearboxes and generators is due to fatigue loading caused by unsteady wind, which reduces the life of the components. This failure increases the maintenance cost and decreases the annual energy production of the turbine.

The reliability of a wind turbine can be improved by replacing the gearbox with a hydrostatic transmission (HST). An HST is one type of high power density continuous variable transmission. HSTs are simple, light and cost effective. They are commonly used in off road construction equipment. The slight compressibility of the hydraulic fluid in an HST reduces the shock loading on mechanical components increasing their life. Because it is continuously variable, an HST decouples the generator speed from the rotor speed, allowing the generator to run at synchronous speed with time varying wind speeds. This eliminates expensive power converters [5] [6].

The University of Minnesota test bed is focused on using a hydrostatic transmission on smaller wind turbines typically used in community wind. It is capable of generating 100 kW with a maximum pressure of 350 bar with 55 kW of electrical input. The test bed has a single pump and motor and is equipped with multiple sensors to accommodate and test a variety of hydraulic fluids, components and controls. The novelty of the paper is use of an advanced control valve to characterize the hydraulic components of the test bed.

This research compliments the HST wind turbine research at RWTH Aachen University. The RWTH test bed has a power level of 1 MW and uses multiple pumps and motors. The RWTH control approach emphasized the switching of pumps and motors to maximize the efficiency at different power levels [7] [8].

## 2 Power Regenerative Hydrostatic Test Platform

### 2.1 Hydrostatic Transmission

In its simplest form, a hydrostatic transmission consists of a hydraulic pump driving a hydraulic motor. The proposed HST for a wind turbine is shown in Figure 1 consisting of a fixed displacement pump and a variable displacement motor. This choice takes advantage of commercially available hydraulic components, control simplicity, transmission efficiency and cost, and is therefore the most practical solution. A closed circuit HST is chosen, eliminating the need for a bulky reservoir. To measure the efficiency and performance of an HST wind turbine, a power regenerative wind turbine test bed has been built at the University of Minnesota.

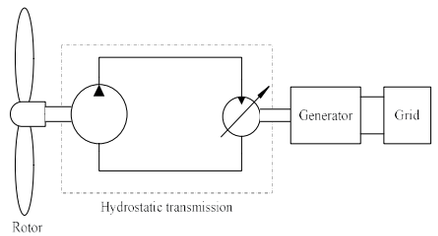


*Figure 1: Schematic of HST wind turbine*

### 2.2 Hydrostatic Wind Turbine Test Bed

The power regenerative research platform consists of two closed loop hydrostatic circuits as shown in Figure 2. The block in dark gray is the hydrostatic transmission under investigation. The block in light gray is the hydrostatic drive (HSD), to simulate the rotor driven by time varying wind.

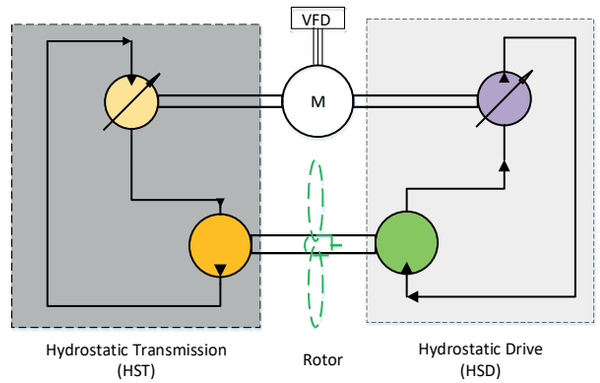


*Figure 2: Schematic of power regenerative test bed*

In the power regenerative test bed, the output power from the HST is fed back into the input of the HSD. A variable frequency drive (VFD) electric motor is coupled to the turbine output shaft to compensate for the losses of the HST and HSD. The VFD regulates the speed of turbine output shaft speed to simulate grid conditions. The power regenerative test platform is shown in Figure 3.

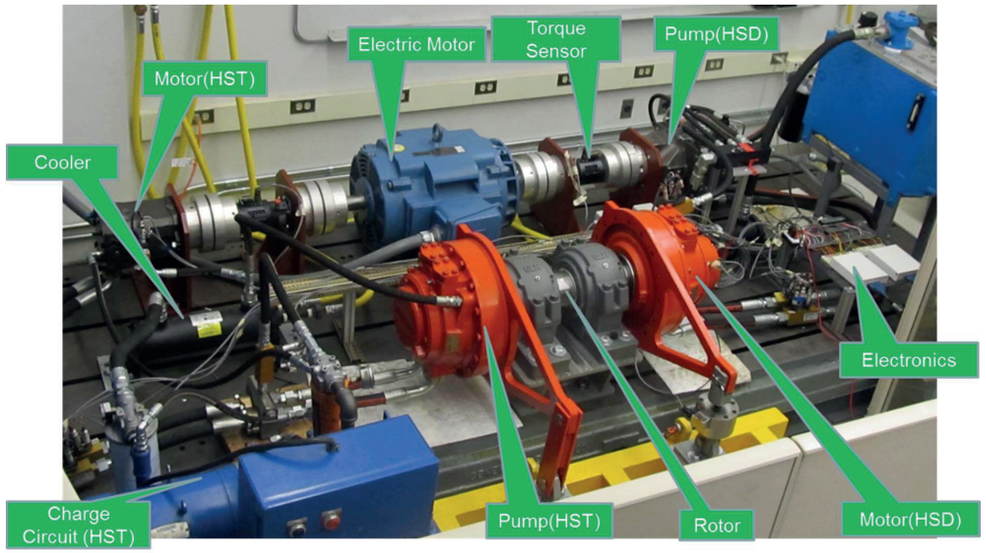


*Figure 3: Power regenerative test bed*

The HSD of the test platform consists of a variable displacement axial piston pump and a fixed displacement radial piston motor. The HST consists of fixed displacement radial piston motor used as a pump and a variable displacement axial piston. Torque and speed sensors have been installed in the high speed (1800 rpm) and low speed (rotor) shaft to measure shaft torque and speed. Pressure, flow and temperature sensors have been installed in all hydraulic lines. An advanced electro hydraulic valve with independent metering is used to calibrate the hydraulic sensors and to characterize the performance of the pump and motors.

## 3 Advanced Control valve

The Advanced Control Valve (ACV) is a CAN enabled electrohydraulic sectional valve with independent metering spool valves. It is capable of controlling either flow or pressure using pressure and spool position sensors, on-board electronics and an advanced control algorithm that delivers high precision and fast response. For pressure and position control the precision is determined by the accuracy of the sensor. Since the flow is not directly measured, the precision for flow control is determined by a calibrated lookup table. For 15 cSt hydraulic oil, the valve has a bandwidth of 17.5 Hz and a rise time of 24 ms. The ACV is shown in Figure 4.

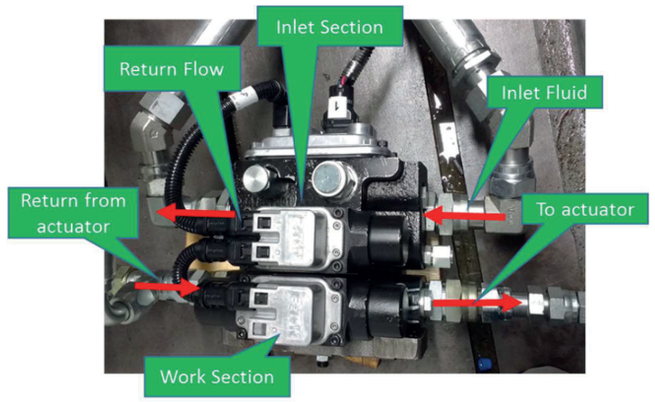


*Figure 4: Advance Control Valve*

This commercial ACV (Eaton CMA200) is integrated in to the power regenerative circuit to calibrate flow sensors and characterize each hydraulic pump and motor. The schematic of the ACV is shown in Figure 5 with inlet section on the left and work section on the right.

The inlet section is connected to the HST pump. The inlet section has a pilot valve that gets its commands from the controller and controls a main stage valve to maintain the inlet pressure. It also has a pressure relief valve that is set at the maximum operating pressure to keep the system safe. The inlet section is connected to a work section valve.

The work section is comprised of two independent spools. The independent pilot spools control the each main stage valve that has its own position sensor for precise operation as shown in Figure 5. The two spools can be controlled as a pair or separately. This allows us to control the inlet A and return B ports of the work section independently. Pressure sensors are located in the A, B, pressure and tank lines. The pilot spool of the work section gets its command from the controller. With the upstream and downstream pressure information and the pilot command, the mainstage spools are moved to create the appropriate orifice area for the desired flow rate. Although the ACV can be used in a wide range of applications, in the wind power test bed it is used to control the pressure of the inlet section to load the pump and control the output flow of the work section.

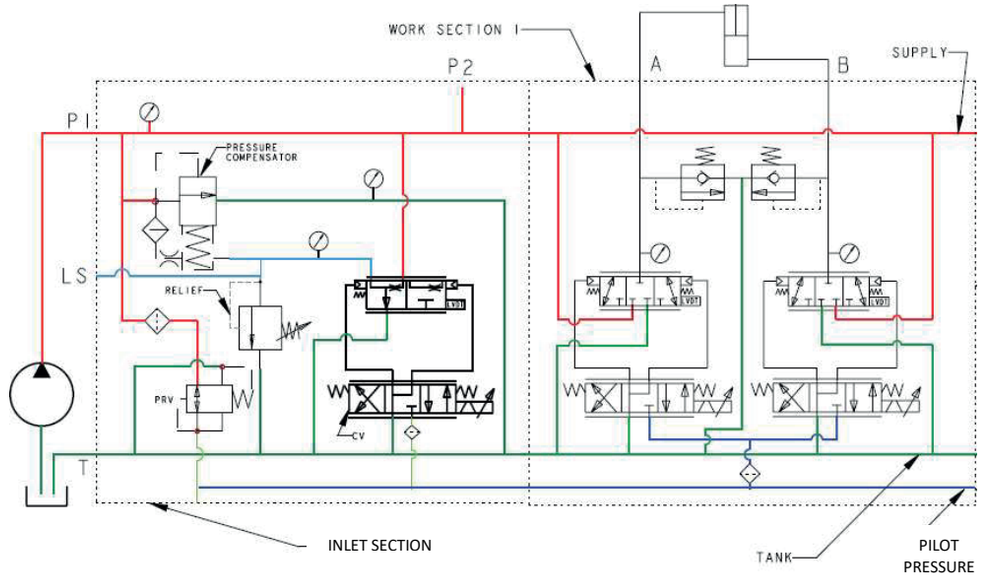


*Figure 5: Schematic of Advanced Control Valve with inlet section (left) and outlet section (right)*

## 4 Calibration of sensor

The hydraulic line of the power regenerative test bed is connected to pressure, temperature and flow sensor modules. The main lines of the HSD and HST are measured with a 15-300 lpm flow sensor, while case drain lines of HST are measured with 8-150 lpm flow sensors. The ACV is used to calibrate all flow sensors on the test bed. The schematic of flow sensor calibration is shown in Figure 6(a). The inlet section of the ACV is connected to the HST pump and the work section is connected to the calibrated flow sensor and test flow sensor in series. While one of the spools in the working section is commanded to control the flow, the other one is commanded to the fully open position to minimize any pressure drop in the returning fluid from the flow sensor. As fluid passes through the orifices, frictional dissipation produces heat. A small volume of fluid is bled out from the circuit and passed through a heat exchanger to reduce the temperature. A charge pump is used to make up for the losses of the fluid on the testing side.

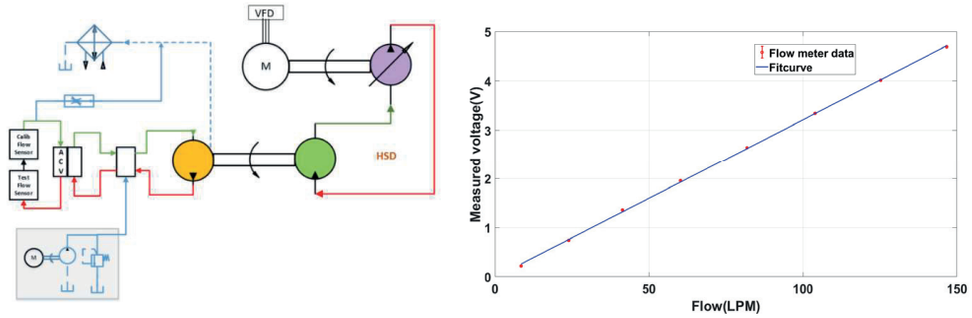


*Figure 6: (a) Schematic flow calibration. (b) Flow sensor data*

The HST pump is driven by the HSD of the power regenerative platform. The pressure of the inlet section of the ACV is set to 60 bar. The ACV does not measure the flow but rather it controls the flow by controlling the position of the spool. A calibrated flow sensor is used to measure the flow of the work section. The output voltage of the test flow meter is collected in the data acquisition system of the wind turbine test platform. The flow sensor data of a 8-151 LPM flow sensor is shown in Figure 6(b) with the calibrated flow measurement in x-axis and the output voltage of the test flow meter in y-axis. A straight line is fit through the data points to compute the gain and bias of the sensor.

The pressure sensor of the module is calibrated with a dead weight tester. The temperature sensors are calibrated using a water bath and calibrated temperature sensors.

## 5 Characterization of components

The testbed has two pumps and two motors. Each pump and motor unit has been characterized on the testbed using the ACV. The inlet section of the ACV is connected to the HST pump to load the HSD motor. The schematic of the test bed for characterization of the hydraulic unit is shown in Figure 7(a). The work section of the ACV is connected to the HST motor. The HST motor is coupled to the high speed shaft. Both electric motor and HST motor drive the HSD pump. The torque and speed sensors are mounted in between the electric motor and the HSD pump to measure the mechanical input power to the HSD pump. Pressure sensors have been installed at each port to measure port pressure of the pump and motor as shown in Figure 7(b). A flow sensor module consisting of flow, pressure and temperature sensors has been mounted in each hydraulic line.

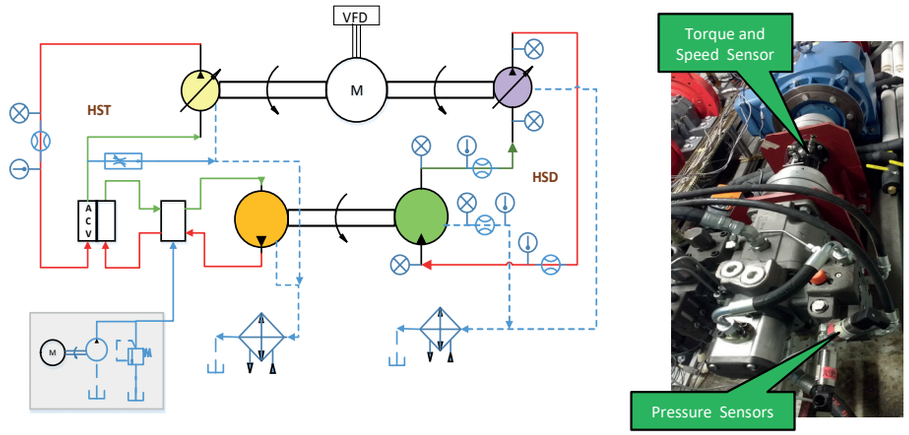


*Figure 7: (a) Schematic of the test bed for characterization of the pump and motors. (b) Speed, torque and pressure sensors on HSD pump.*

A certain volume of fluid is directed from the low-pressure line of the HST motor to a heat exchanger to compensate for the heat generated by the metering of the ACV. The temperatures of the hydraulic oil (ISO 68) in both the HSD and HST are maintained at 40 degrees C. The performance of the HSD pump and motor of the power regenerative test bed is discussed in this paper.

### 5.1 HSD pump

A variable displacement axial piston pump with maximum pump displacement ($D_p$) of 160 cc/rev is used in the HSD circuit. For wind turbine applications, the HSD pump rotates at a constant speed ($\omega_p$). The pump output flow ($Q_p$ ) is varied by changing the swashplate angle. The position of the swashplate angle is changed by a servo valve. $x$ is the displacement fraction of the pump. The volumetric efficiency ($\eta_{p\_vol}$) of the pump is given by Equation (1). .

$$\eta_{p\_vol} = \frac{Q_p}{xD_p\omega_p} \tag{1}$$

The volumetric efficiency of the HSD pump at 1000 RPM is shown in Figure 8(a). The pump shows nearly constant efficiency at higher displacement fractions. However, there is a sharp decrease in volumetric efficiency below 30% displacement fraction. As pressure increases the leakage flow through the orifice increases and hence volumetric efficiency decreases.

The mechanical performance of the pump is computed by measuring the pressure at the high pressure port ($P_{p_{hp}}$) and the low pressure port ($P_{p_{lp}}$). The torque ($T_p$) applied to the pump is measured by a rotary torque sensor. The pressure difference across the port has been created by loading the pump by ACV. The mechanical efficiency of the pump is given by Equation (2).

$$\eta_{p\_mech} = \frac{xD_p(P_{p_{hp}} - P_{p_{lp}})}{T_p} \tag{2}$$

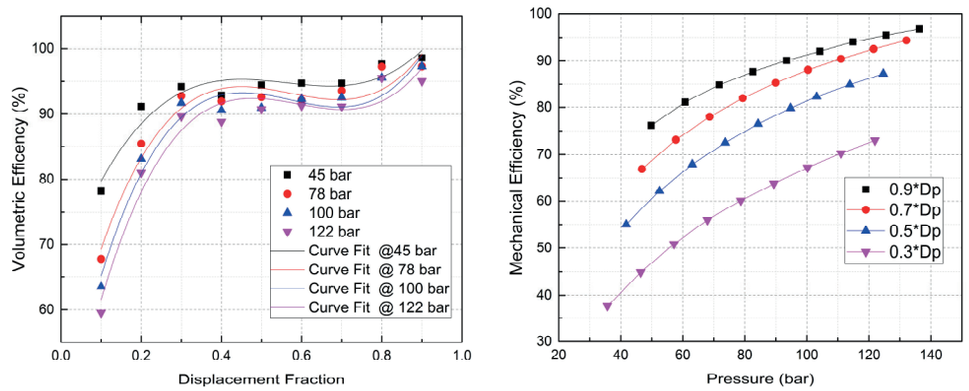


*Figure 8: (a) Volumetric efficiency of the HSD pump at different pressures. (b) Mechanical efficiency of the HSD pump at different displacement fractions.*

The mechanical efficiency of the pump with respect to the pressure difference ($P_{p_{hp}} - P_{p_{lp}}$) and displacement fraction is shown in Figure 8(b). The mechanical efficiency is proportional to the pressure difference. However, the efficiency of the variable displacement pump decreases with decreases in displacement fraction.

### 5.2 HSD Motor

In the power regenerative test bed, the HSD motor is used to emulate a low speed and high torque wind turbine rotor. A fixed displacement radial-piston type motor with a motor displacement ($D_m$) of 2512 cc/rev has been used in the testbed. The input flow ($Q_p$) to the motor is measured at its inlet port. The motor is connected to the rotor shaft through the hollow shaft of the cylinder block. The rotor speed ($\omega_r$) is measured by a speed encoder mounted at the shaft end. The volumetric efficiency ($\eta_{m\_vol}$) of the motor is given by Equation (3).

$$\eta_{m\_vol} = \frac{D_m \omega_r}{Q_p} \tag{3}$$

The volumetric efficiency of the motor with respect to pressure and speed is shown in Figure 9(a). As the port pressure increases, the leakage through the orifice increases, thereby decreasing the efficiency. The efficiency also increases with increase in rotor speed.

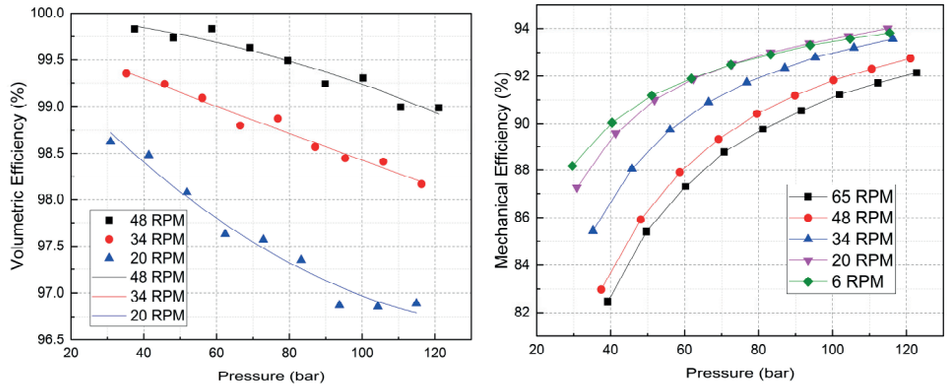


*Figure 9: (a) Volumetric efficiency of the HSD motor at different pressure and speed (b) Mechanical efficiency of the HSD motor at different pressure and speed.*

The mechanical torque ($T_r$) is transmitted to the rotor shaft through the splines. The torque is computed from the load cell measurement of the motor torque arm. The port pressure at the inlet ($P_{m_{hp}}$) and outlet ($P_{m_{lp}}$) of the motor has been measured. The mechanical efficiency ($\eta_{m\_mech}$) of the motor is computed by Equation (4).

$$\eta_{m\_mech} = \frac{T_r}{D_m(P_{m_{hp}} - P_{m_{lp}})} \tag{4}$$

The mechanical efficiency of the HSD motor is shown in Figure 9(b). The efficiency of the motor decreases with decreasing port pressure. With increasing rotor speed, the velocity of the piston increases and hence frictional loss between cylinder and piston increases. Due to increases in frictional loss, the mechanical efficiency decreases.

## 6 Summary and Conclusion

The electrohydraulic advanced control valve is equipped with multiple sensors, on-board electronics and an advanced control algorithm that delivers high precision and fast response. The ACV is integrated with in to the power regenerative test platform to calibrate flow sensors and measure the performance of each hydraulic component. The ACV provides a flexible architecture to characterize hydraulic pumps and motors by using the existing power of the testbed. In both the pump and motor, mechanical efficiency increases with increasing pressure but volumetric efficiency decreases. The volumetric efficiency of the motor is around 99% during high-speed operation. The pump and motor performance at higher pressure and higher speed will be evaluated in the future.

## 7 Acknowledgements

This project is funded by the National Science Foundation under grant #1634396. We also thank Eaton, Linde, Danfoss, Bosch Rexroth, Flo-tech and ExxonMobil for donating the components for the test bed. We are thankful to our summer undergraduate researchers Christina Geiser, Diana Luc and Yida Niu for working on calibration of sensors, data acquisition and temperature control of the test platform. We are also grateful to graduate students in our lab, Daniel Escobar and Yuhao Feng for helping us in setting up the experiments.

## Nomenclature

| *Variable* | *Description* | *Unit* |
|---|---|---|
| T | Torque | [Nm] |
| $P$ | Pressure | [bar] |
| $\eta$ | Efficiency | [-] |
| $D_p$ | Pump Displacement | [m3/rev] |
| $D_m$ | Motor Displacement | [m3/rev] |
| $Q$ | Flow | [m3/sec] |
| ω | Angular Speed | [rad/sec] |
| χ | Displacement Fraction | [-] |

## References

/1/ World wind energy association report, www.wwindea.org

/2/ Wind vision report by Department of Energy, www.energy.gov

/3/ Sheng, S., Report on wind turbine subsystem reliability- a survey of various databases. National Renewable Energy Laboratory, Golden, CO, Tech. Rep. NREL/PR-5000-59111, 2013.

/4/ Lange, M., Wilkinson, M., and Thomas van Delft, T. V., Wind turbine reliability analysis. DEWEC, Bremen, 2011.

/5/ Thul, B., Dutta, R., Stelson, K. A., Hydrostatic transmission for mid-sized wind turbines, 52nd National Conference on Fluid Power, Las Vegas, USA, 2011.

/6/ Dutta R., Wang F., Bohlmann B.F., Stelson K.A. Analysis of short-term energy storage for midsize hydrostatic wind turbine. Journal of Dynamic Systems, Measurement, and Control. 2014 Jan 1; 136(1):011007.

/7/ Schmitz, J., Vatheuer, N., & Murrenhoff, H. (2011). Hydrostatic drive train in wind energy plants. RWTH Aachen University, IFAS Aachen, Germany.

/8/ Schmitz, J., Diepeveen, N., Vatheuer, N., & Murrenhoff, H. (2012). Dynamic transmission response of a hydrostatic transmission measured on a test bench. EWEA.